Supplementary Figures

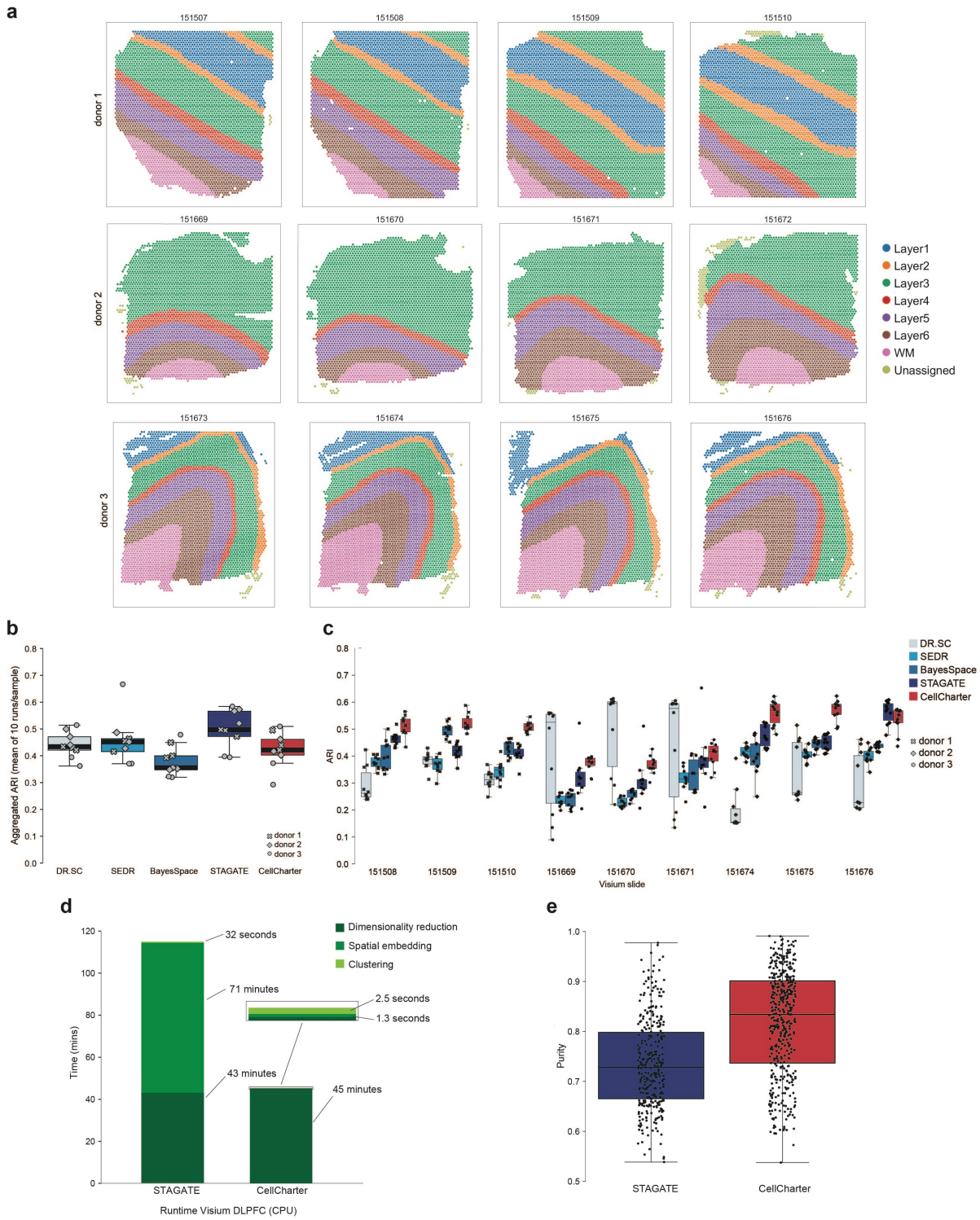

Supplementary Figure 1: Benchmarking of spatial clustering methods

a) Manual annotations of the Visium DLPFC samples. **b)** Mean ARI for each DLPFC sample (over 10 repetitions) obtained by the listed methods upon performing individual spatial clustering of the samples (n = 9 samples). **c)** ARI for each DLPFC sample obtained by the listed methods upon performing joint clustering of all samples (n = 9 samples). **d)** Runtime divided by processing step of the two best-performing methods (STAGATE and CellCharter) in clustering all 12 samples of DLPFC on CPU. **e)** Purity of the cluster components in the CODEX mouse spleen dataset for the clusters of the two best-performing methods.

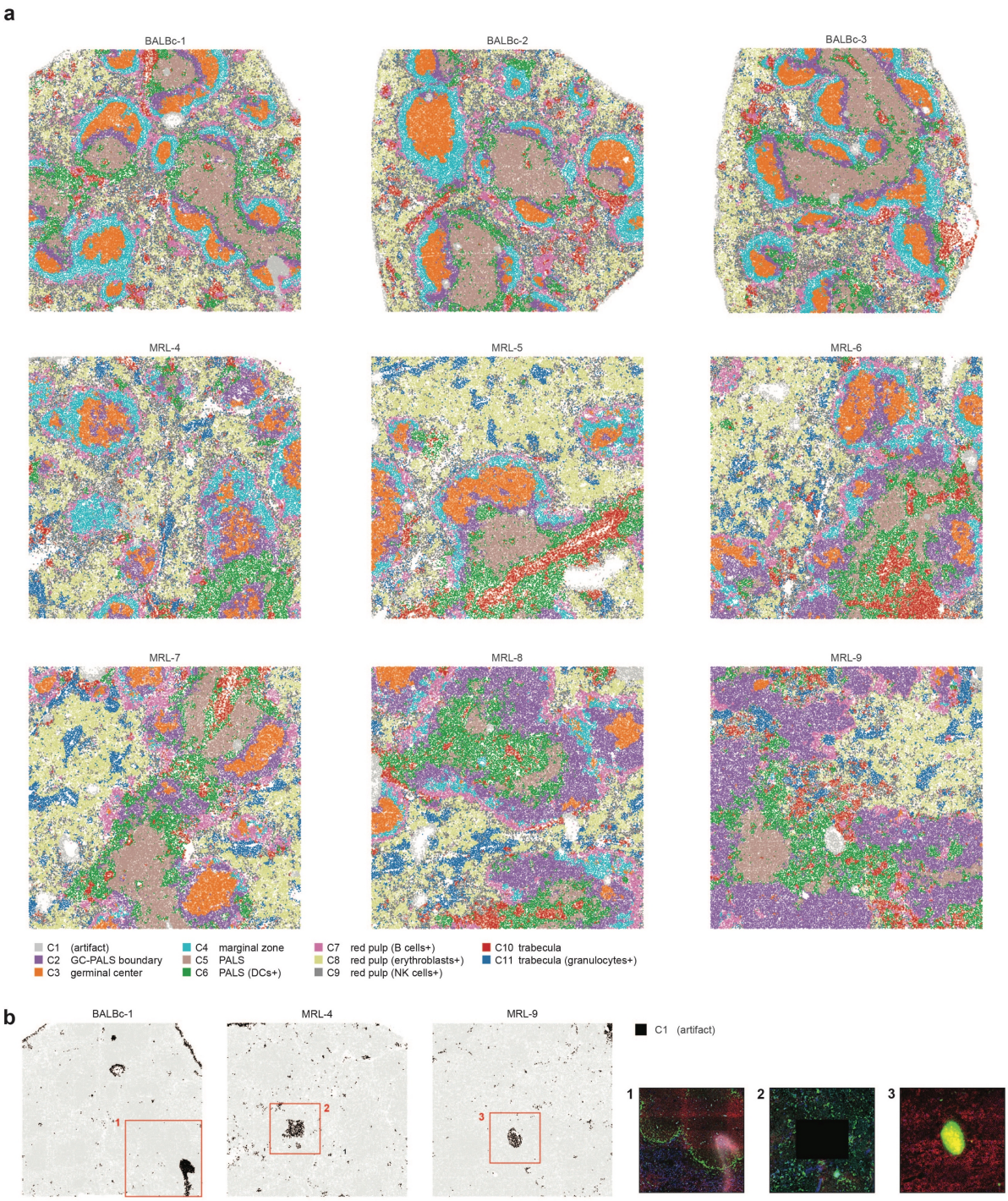

Supplementary Figure 2: Characterization of CellCharter's spatial clusters of the CODEX mouse spleen dataset.

a) CellCharter's spatial cluster at n = 11 clusters for all cells of the 3 healthy (BALBc) and 6 systemic lupus erythematosus samples (MRL). **b)** Examples of staining and imaging artifacts associated with cluster C1.

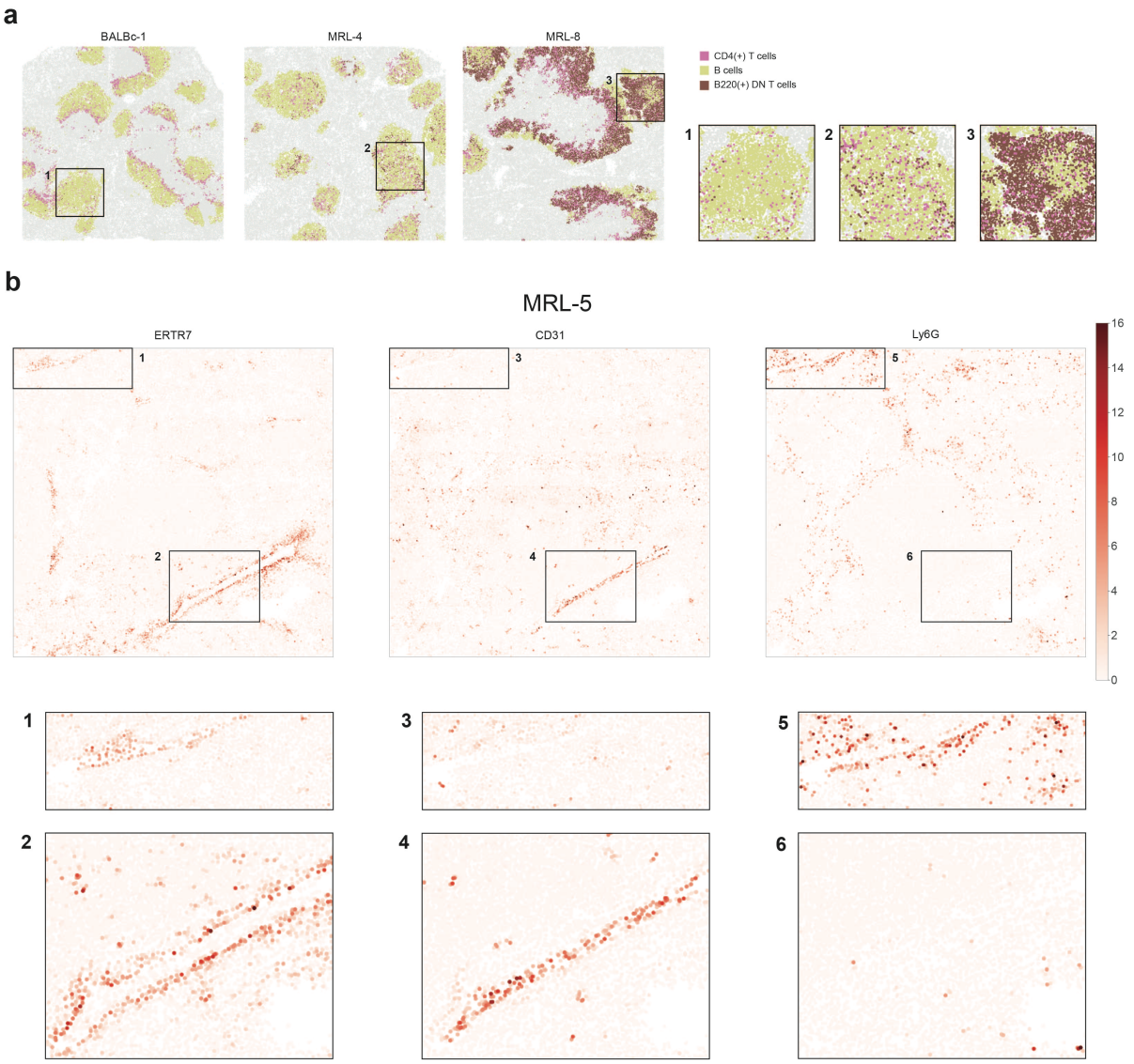

Supplementary Figure 3: Differences in the spatial organization between healthy and systemic lupus spleen.

a) Spatial distribution of $CD4^+$ T cells, B cells, and $B220^+$ T cells in the clusters associated to the germinal center, marginal zone, and GC-PALS boundary for representative examples of healthy (BALBc-1), early lupus (MRL-4) and intermediate lupus (MRL-8) spleen. **b)** Normalized intensity of ERTR7, CD31, and Ly6G markers in the intermediate lupus sample MRL-5. The MRL samples show the presence of two distinct clusters associated with trabecular structures. Insets (1 to 6) highlight the different expression of the markers in correspondence trabecular clusters C10 (insets 2, 4, 6) and C11 (insets 1, 3, 5).

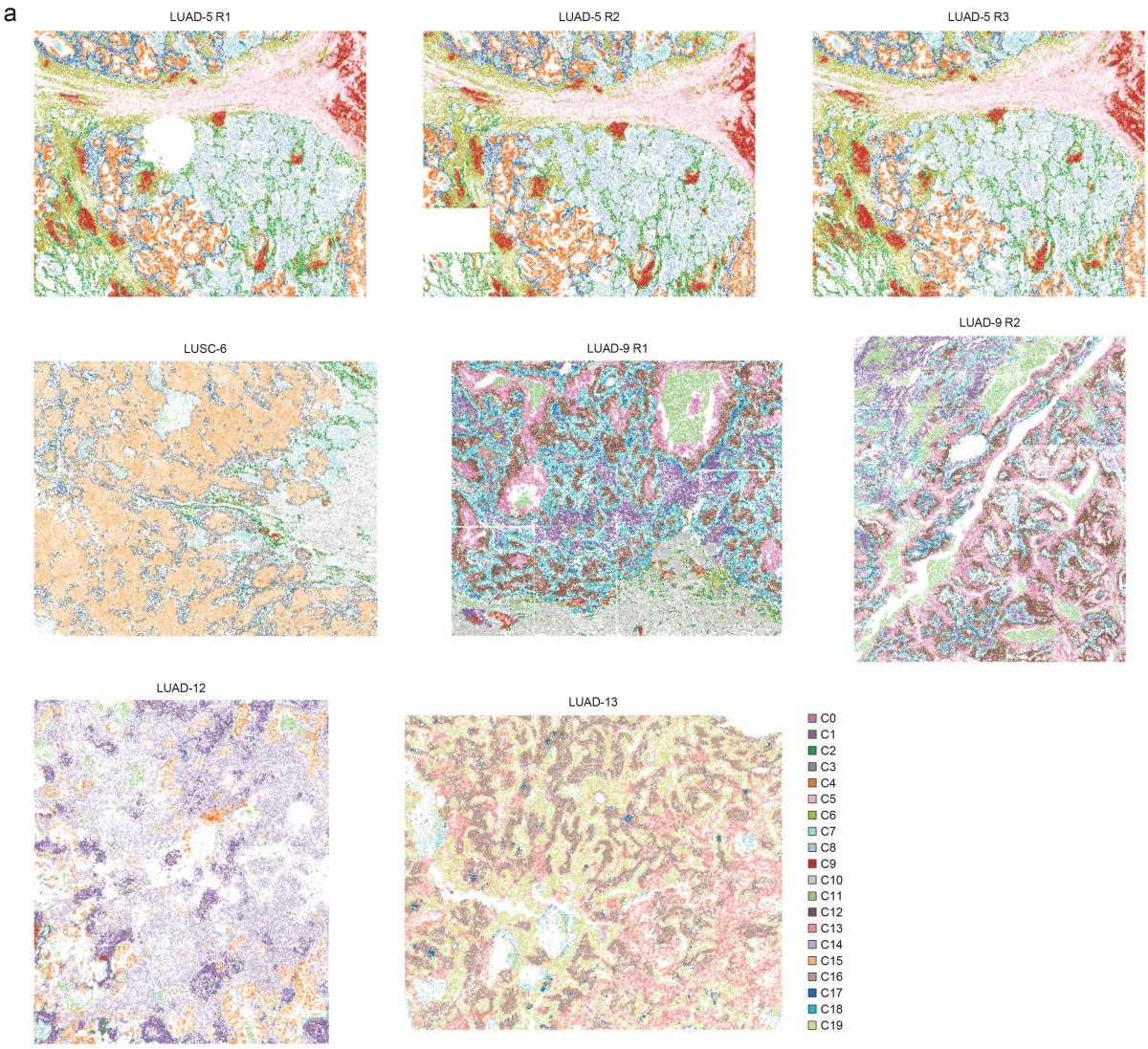

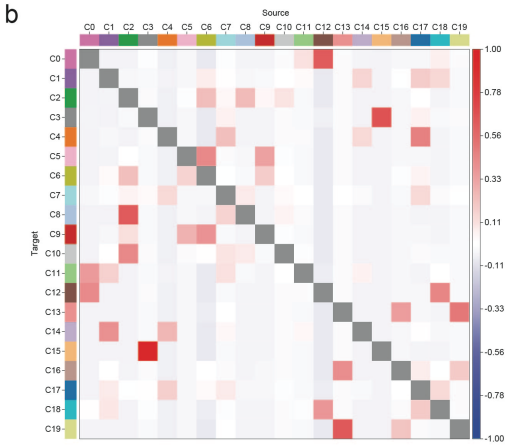

Supplementary Figure 4: Characterization of CellCharter's spatial clusters of the CosMx NSCLC dataset.

a) CellCharter's spatial cluster at n = 20 clusters for all cells of the CosMx NSCLC samples.

b) Cluster neighborhood enrichment between the spatial clusters in all samples.

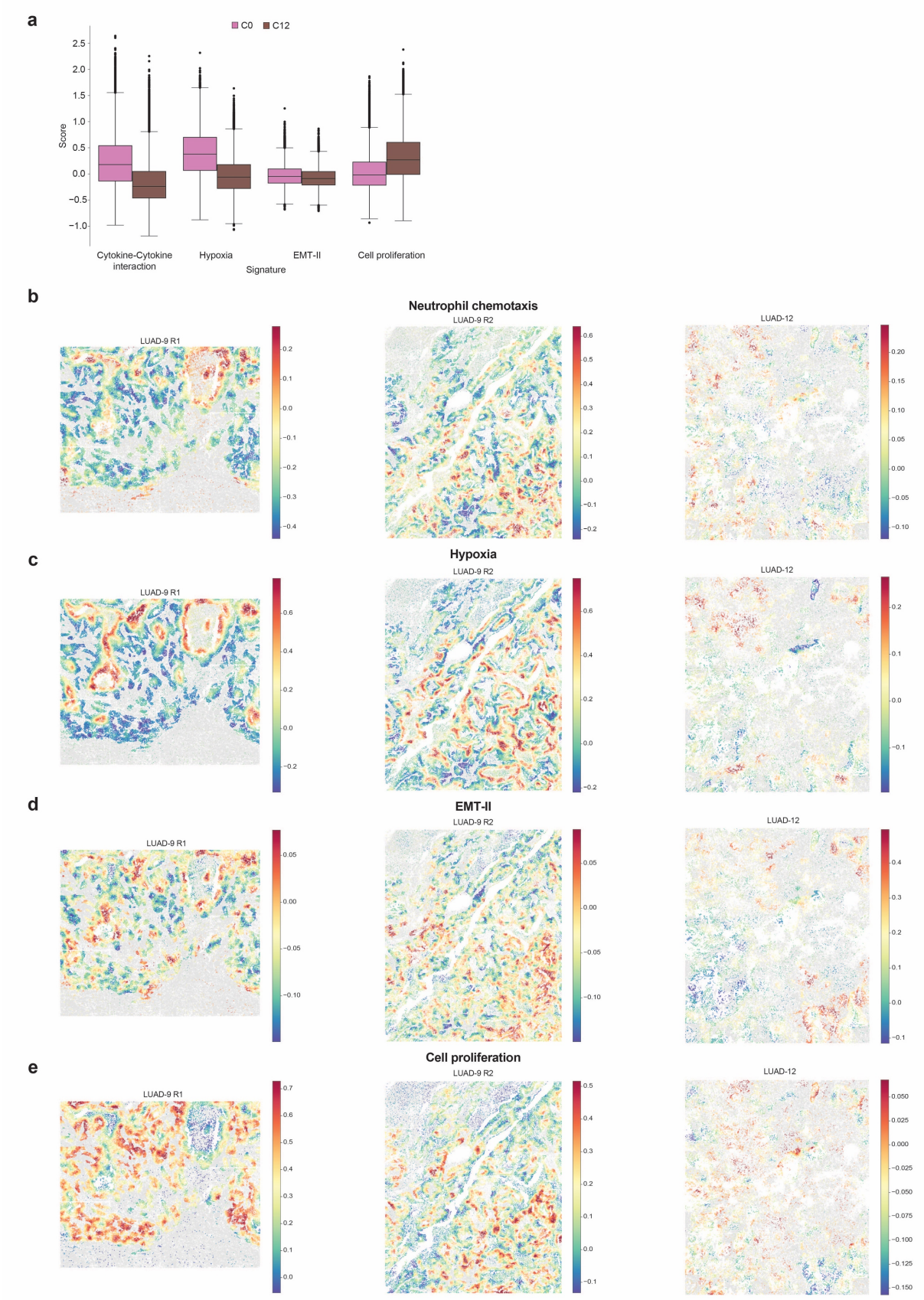

Supplementary Figure 5: Cell signature scores in two NSCLC patients

a) Gene expression signature score of tumor cells in spatial clusters C0 and C12. **b-e)** Gene expression signature score of tumor cells of patients LUAD-9 and LUAD-12 for four gene signatures.

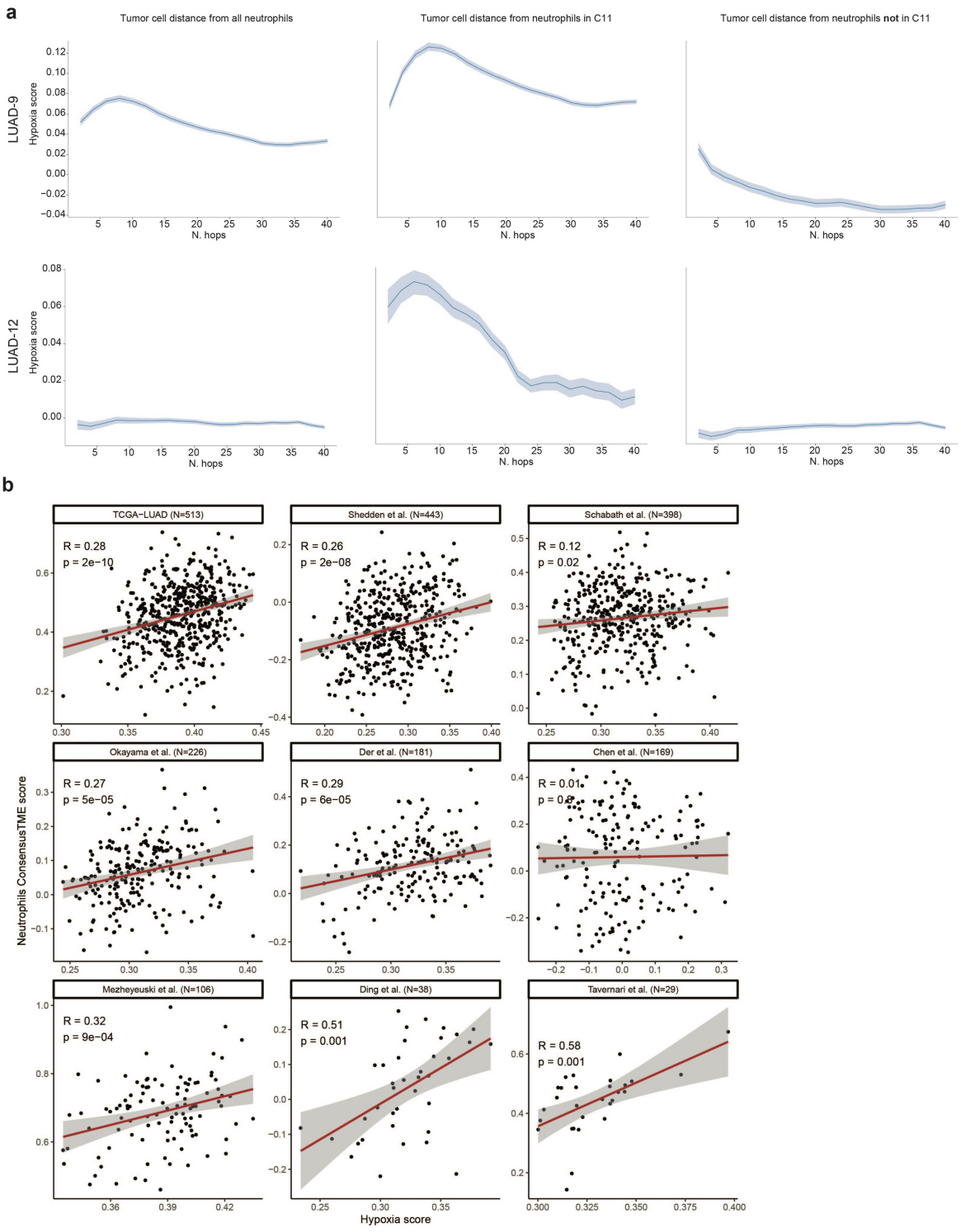

Supplementary Figure 6: Association between tumor hypoxia and neutrophil infiltration **a)** Average hypoxia gene signature score for tumor cells at increasing hop-distance from all neutrophils (left), neutrophils assigned to spatial cluster C11 (center), and neutrophils not assigned in cluster C11 (right). **b)** Correlation between hypoxia gene signature score and neutrophil infiltration in 9 bulk RNA-seq datasets of lung adenocarcinoma.

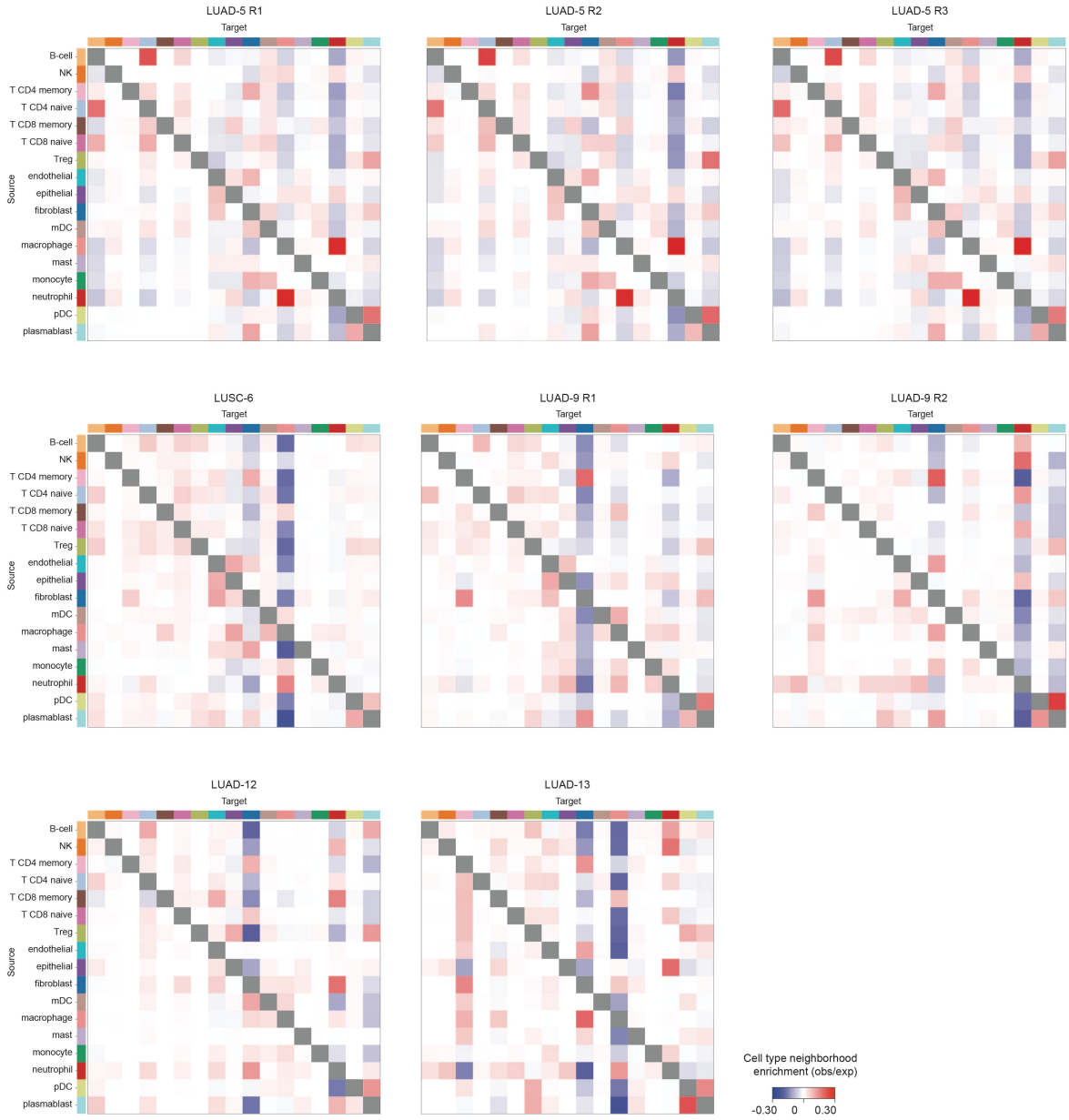

Supplementary Figure 7: Proximity between non-tumor cell types in NSCLC patients
Cell type neighborhood enrichment among all non-tumor cell types for each CosMx NSCLC sample.